Intrinsic Allosteric Inhibition

DOI: 10.1002/anie.201305741

Intrinsic Allosteric Inhibition of Signaling Proteins by Targeting Rare Interaction States Detected by High-Pressure NMR Spectroscopy**

Hans Robert Kalbitzer, Ina C. Rosnizeck, Claudia E. Munte, Sunilkumar Puthenpurackal Narayanan, Veronika Kropf, and Michael Spoerner*

Proteins involved in signal transduction exist in more than one conformational state and thus generally permit a new type of allosteric inhibition by targeting their rare interaction states. An example is the Ras protein where the protein–protein interaction of Ras with effectors can be modulated by small compounds that bind to the conformational state 1(T). An analysis of the Ras cycle predicts at least eight drug-relevant functional states of the protein that can be used for an allosteric modulation of the Ras activity. We were able to identify the four states expected in activated Ras by high-pressure NMR spectroscopy. The study focused on the Ras system leads to a novel, generally applicable strategy for the development of allosteric inhibitors of protein–protein interactions in multiple-state systems typical for signaling proteins.

The Ras protein is permanently activated in approximately 30% of all human tumors by specific point mutations.[1] It is the prototype member of the Ras superfamily with more than 100 different guanine nucleotide-binding (GNB) proteins of different sub-families (see for example Ref. [2]). The GNB proteins cycle between two main structural states, stabilized by GDP and GTP, respectively. In the GDP-bound state (Figure 1a), the affinity to effectors is low. In this simple model, the affinity to effector proteins of the GTP-bound state is high and the signal induced by the exchange of GDP to GTP by the guanine nucleotide exchange factors (GEFs) can be transmitted. The activation cycle is finished by GTP hydrolysis, which is catalyzed by GTPase activating proteins (GAPs). As activated Ras has to interact with three different proteins with quite different interaction sites, fundamental thermodynamical considerations require that at least three conformational states of the activated GNB protein Ras·Mg^{2+}·GTP must coexist in solution,[3] states that correspond to the complexes with GEFs (state 1(T)), effectors (state 2(T)), and GAPs (state 3(T); Figure 1).

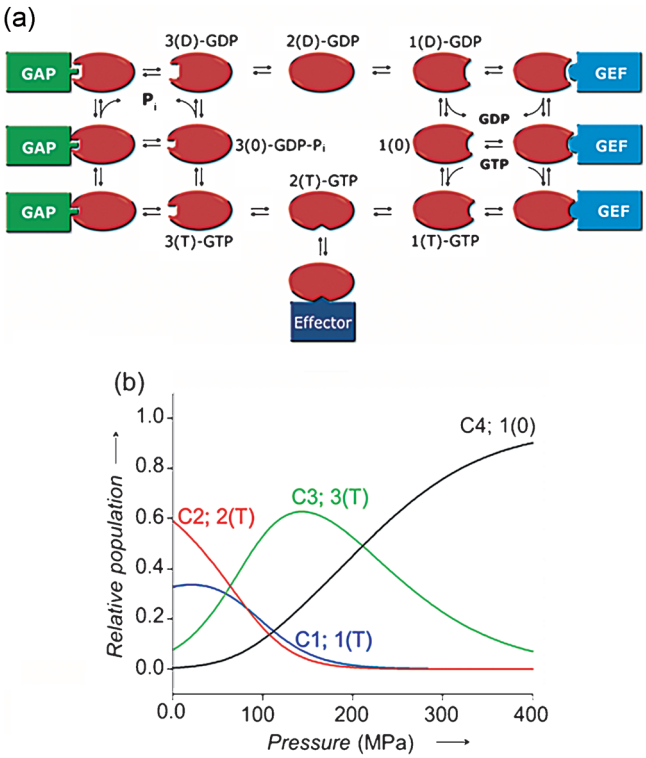

Figure 1. Conformational states of Ras during the signaling cycle. a) General model of functional states of Ras that are potential drug targets. Note that additional druggable states still exist; a well-known example is the manipulation of the covalent modifications of the C-terminus. b) The relative populations of the different conformational states from C1 to C4 were calculated with the parameters given in Table 1 as function of pressure. C1 corresponds to state 1(T), C2 to state 2(T), and C3 and C4 probably to state 3(T) and state 1(0).

Two of the main conformational states (state 1(T) and state 2(T)) of Ras·Mg^{2+}·GppNHp can be directly observed by ^{31}P NMR spectroscopy and are characterized by different chemical shift values for the resonances of the α- and γ-phosphate groups.[4–6] It has been shown earlier by NMR spectroscopy as well as kinetic experiments that Ras can interact only in state 2(T) with the Ras binding domains (RBD) of effector proteins such as RalGDS, cRaf-1, Af6, and Byr2 with high affinity.[4–9] In contrast, the guanine nucleotide exchange factor Sos interacts preferentially with state 1(T).[3] In the nucleoside diphosphate complexed form (D) the

[*] Prof. Dr. H. R. Kalbitzer, Dr. I. C. Rosnizeck, Prof. Dr. C. E. Munte,[+] Dr. S. P. Narayanan, V. Kropf, Priv.-Doz. Dr. M. Spoerner
Institute of Biophysics and Physical Biochemistry, Centre of Magnetic Resonance in Chemistry and Biomedicine (CMRCB), University of Regensburg
Universitätsstrasse 31, 93047 Regensburg (Germany)
E-mail: Hans-Robert.Kalbitzer@Biologie.Uni-Regensburg.de

[+] Present address: Physics Institute of São Carlos, University of São Paulo
Av. Trabalhador Sãocarlense 400, 13566-590 São Carlos, SP (Brazil)

[**] This work was supported by the Deutsche Forschungsgemeinschaft (DFG), the Bayerische Forschungsstiftung (BFS), and the Human Frontier Science Program Organisation (HFSPO). Part of the work has been presented at the EUROMAR 2012 in Dublin, Ireland.

Supporting information for this article, including sample preparation, the NMR spectroscopy, and the evaluation of the high-pressure data, is available on the WWW under http://dx.doi.org/10.1002/anie.201305741.

corresponding GEF and GAP interacting states 1(D) and 3(D) should exist besides the main conformational state 2(D). In fact, by ^{31}P NMR, two conformational states could already be identified for Ras·Mg^{2+}·GDP.[10] The minimum Ras cycle also requires a nucleotide free state and a state with GDP·P_i bound that we call 1(0) and 3(0) in the following (Figure 1).

For the experimental detection of additional conformational states in the Ras protein, we performed high-pressure [^{1}H,^{15}N]-HSQC experiments on Ras complexed with the non-hydrolysable GTP analogue GppNHp (Supporting Information, Figure S1). A fit of the pressure-induced chemical shifts by a second order Taylor expansion (Supporting Information, Eq. (1)) has been used to identify those regions of the protein that are particularly pressure-sensitive. ^{1}H and ^{15}N NMR chemical shifts were corrected for pressure-induced random-coil effects[11] and thus show only specific pressure effects (Supporting Information, Figures S2, S3). The pressure coefficients can be mapped on the structure of Ras·Mg^{2+}·GppNHp (Figure 2; Supporting Information, Figure S3). Residues interacting with published drugs are indicated.[12–15]

Qualitatively, large pressure coefficients can be associated with large structural changes in the vicinity of the atom under consideration, although missing shift changes do not necessarily mean the absence of structural changes.

Along with chemical shift changes, changes of the cross-peak volumes can also be observed (Supporting Information, Figure 3, Figure S4). Under slow-exchange conditions, a change of the cross-peak volumes can be expected when in an *N*-site equilibrium the population of the observed conformational state changes with pressure. For most cross-peaks, the intensity decreases, as the population of the main state 2(T) decreases but also new cross-peaks appear with pressure (for example Gly12; Supporting Information, Figure S5). The volume changes can be plotted on the surface of the state 2(T) structure of Ras (Figure 2b).

The pressure-sensitive regions can be compared with the interaction sites of Ras in complexes with GEFs, effectors, and GAPs (Supporting Information, Figure S6). In the conformational selection model (Figure 1), parts of these regions are expected to be involved in conformational transitions and therefore should be detectable by pressure perturbations. Figure 2 demonstrates a good correlation with these data. However, the conformational transitions should not be restricted to the interaction surface only, as structural elements in a protein are strongly coupled. Indeed, also outside the interaction surface pressure significant effects are observed. This is especially evident on the backside of the protein (Figure 2), where for example Gln43 and Thr50 show a very large pressure response.

A more detailed analysis of the data with a thermodynamic model (see the Supporting Information) allows the determination of the free-energy difference ΔG_{ij}^0 and the corresponding molar partial volume difference ΔV_{ij}^0 between two conformational states Ci and Cj at a reference temperature T_0 and a reference pressure p_0 (Table 1).

It turns out that at least four different conformational states C1 to C4 are required for a satisfactory explanation (and fitting) of the pressure-induced chemical shift changes. A typical example is shown in Figure 3, where the ^{15}N chemical shift changes of the cross-peak of Glu49 and the volume changes of the cross-peak of Ala18 can be fitted satisfactorily with the same Gibbs free energy and partial molar volume

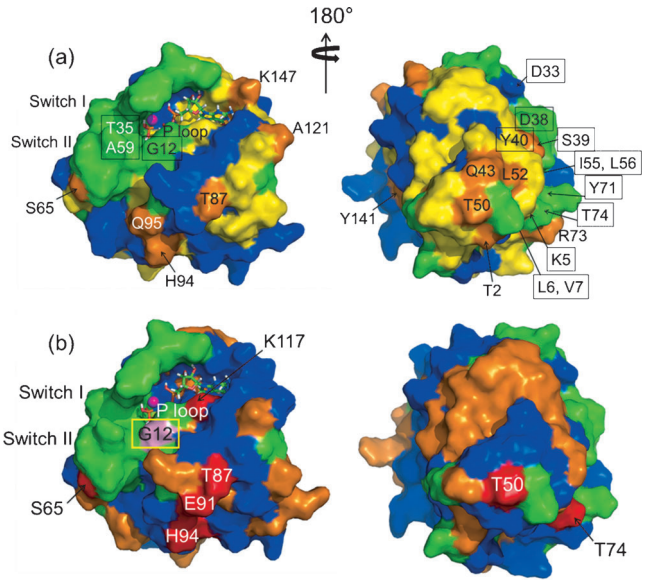

Figure 2. Pressure-sensitive residues in Ras(wt)·Mg^{2+}·GppNHp and protein–protein interaction sites. a) Residues exhibiting large first-order pressure coefficients for the amide protons and amide nitrogen atoms are mapped onto the surface of the crystal structure of Ras(wt)·Mg^{2+}·GppNHp[16] (pdb 5P21). Residues with pressure coefficients $B_{1,2}^* \leq 2\sigma_0$ and at least one in the range $\sigma_0 < B_1^* \leq 2\sigma_0$ are depicted in yellow. Residues with at least one pressure coefficient $> 2\sigma_0$ are depicted in orange. Amino acids, which are not visible in the [^{1}H,^{15}N]-HSQC spectrum of Ras(wt)·Mg^{2+}·GppNHp or could not been followed within the pressure series are shown in green. Residues with $B_{1,2}^* \leq \sigma_0$ are colored blue. Residues characterizing binding sites of Ras-inhibitors are labeled: Zn^{2+}-cyclen, Gly12, Asp33, Thr35, Ala59,[12] Zn^{2+}-BPA, Asp38, Ser39, Tyr40,[13] 4,6-dichloro-2-methyl-3-aminoethyl-indole (DCAI), Lys5, Leu6, Val7, Ile55, Leu56, and Thr74,[14] and 2-((1H-Indol-3-yl)methyl)-3H-imidazo[4,5-*c*]pyridine, Lys5, Val7, Ser39, Asp54, Leu56, Tyr71, Thr74.[15] b) [^{1}H,^{15}N]-HSQC cross-peak volume changes with pressure are plotted on the surface of the crystal structure of Ras(wt)·Mg^{2+}·GppNHp. Residues with a volume reduction by $> \sigma_0$ are colored orange, peaks which completely disappear at 180 MPa are shown in red. Residues which are not visible at ambient pressure owing to exchange broadening are colored green, residues showing peak volume change $< \sigma_0$ are colored blue. At 278 K, the signals of Gly12 and Gly13 become visible at high pressure (colored pink).

Table 1: Conformational transitions and corresponding molar free energies ΔG^0 and molar volumes ΔV^0 of Ras(wt)·Mg^{2+}·GppNHp at 303 K.[a]

Transition	ΔG^0 [kJ mol^{-1}]	ΔV^0 [mL mol^{-1}]
C2→C1	1.5 ± 0.2	−18 ± 1
C2→C3	5.2 ± 0.3	−81 ± 3
C2→C4	12.4 ± 0.4	−115 ± 2

[a] The differences in free energies ΔG^0 and partial molar volumes ΔV^0 for the transitions C2→C1 and C2→C3 are independent of temperature in the range between 278 K and 303 K within the limits of error. ΔG^0 and ΔV^0 were determined from the pressure dependence of chemical shifts and cross-peak volumes.

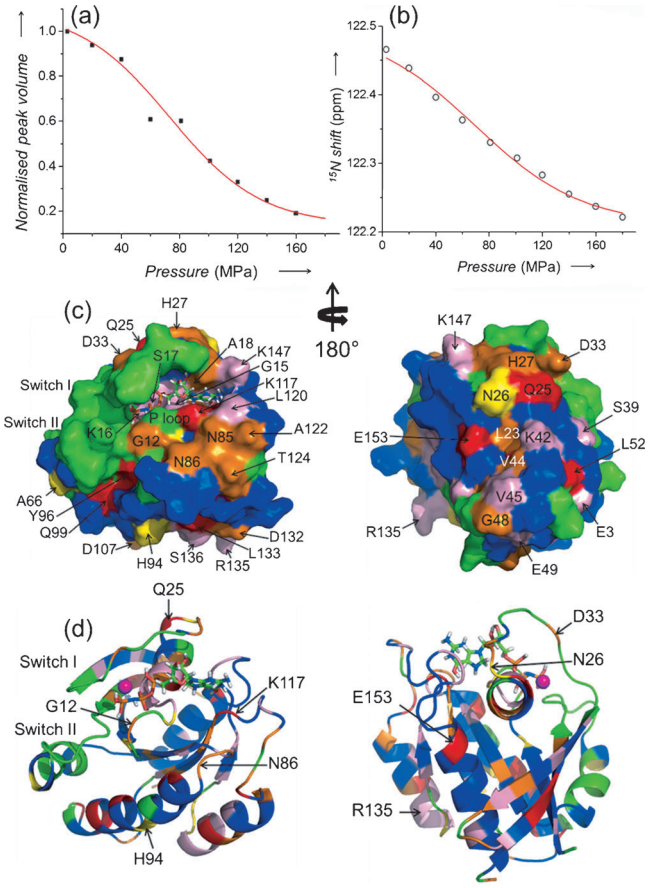

Figure 3. Pressure dependence of conformational transitions. Fit of a) the normalized pressure-dependent volume changes of the cross-peak of Ala18, and b) the $^{15}N^{H}$ chemical shift changes of the amide cross-peak of Glu49 in a [^{1}H,^{15}N]-HSQC spectrum of Ras(wt)·Mg^{2+}·GppNHp assuming slow exchange (Supporting Information, Eqs. (4) and (8)) and fast exchange in the NMR timescale (Supporting Information, Eqs. (2) and (3)), respectively. The temperature was 303 K. Fit parameters for both residues in a two-state model are ΔG_{24} 12.4 kJ mol^{-1} and ΔV_{24} −115 mL mol^{-1}. χ^2 are 0.003 and 0.003, respectively. c) Residues sensing different transitions are depicted on the van der Waals surface calculated from the X-ray structure of Ras·Mg^{2+}·GppNHp.[16] The residues sensing only the transition C2 to C1, C2 to C3, and C2 to C4 are depicted in yellow, orange, and pink, respectively. Residues sensing transitions C2 to C1 and C2 to C3 are colored red. Residues that do not show a significant pressure response are depicted in blue and residues that could not be detected are depicted in green. d) Ribbon model showing the corresponding secondary structure elements.

differences. A number of residues show a biphasic pressure dependence of chemical shifts that is typical (and can be fitted) in a model where more than one transition influences the reporter spin (Supporting Information, Figure S7). From earlier studies, it is clear that the structural states that dominate at atmospheric pressure in the wild-type protein are the effector binding state 2(T) and the exchange factor interacting state 1(T). By ^{31}P NMR spectroscopy we had earlier determined a ΔG_{21}^{0} of 1.48 kJ mol^{-1}[6] and a ΔV_{21}^{0} of −17.2 mL mol^{-1},[3] respectively. Within the limits of error these values are equal to the free energy differences and partial volume differences of the C2–C1 transition obtained herein (Table 1). The nature of conformation C3 and C4 is not clear as such, but from our general minimum model (Figure 1), it is likely that one of these states represents the GAP interacting state 3(T). The fourth state could represent the open, nucleotide-free (low-affinity state for nucleotides) 1(0) (Figure 1), as the nucleotide should be released at very high pressures. In fact, in earlier denaturation studies with GdmCl, the release of the nucleotide was observed by ^{31}P NMR spectroscopy, giving a ΔG^{0} value from state 2(T) to a nucleotide-free state of approximately 9.8 kJ mol^{-1}, a value that is in the range of 12.4 ± 0.4 kJ mol^{-1} estimated here for the C2–C4 transition.[3] State C4 does not represent a completely denatured state, as the ^{1}H NMR spectra still show the typical features of a folded hydrophobic core, such as methyl resonances shifted upfield.

For an analysis of the data in structural terms, the residues influenced by the different transitions are color-coded on the surface of the crystal structure of Ras (Figure 3); a detailed annotation in the sequence of Ras is given in the Supporting Information, Figure S6.

Gly12, His27, Asp33, and Asn86 sense the C2–C3 transition (Table 1) and are part of the GAP interaction site (Supporting Information, Figure S6). This suggests that C3 corresponds to state 3(T) as defined in Figure 1. Gly15, Lys16, Ser17, Ala18, Leu120, Ala146, and Lys147 are selectively sensing the C2–C4 transition; they are known to be involved in the nucleotide binding that should be impaired in state 1(0); thus conformation C4 most likely corresponds to state 1(0) in our model.

From switch I and switch II, the signals of only a limited number of residues is visible in the wild-type protein, and most residues are not or only barely visible at low pressures in the wild type protein. This is most probably due to the occurrence of multiple conformations in intermediate and slow exchange on the NMR timescale ($< 10\ s^{-1}$), having originally been termed as regional polysterism by Ito et al.[17] In fact, many of these residues are located in the overlapping interaction sites of GEFs (state 1(T)), effectors (state 2(T)), and GAPs (state 3(T); Supporting Information, Figure S6). Most of them become visible in the 1(T) mutant Ras(T35S), which in contrast to the wild-type protein exists predominantly in state 1(T) at ambient pressure, confirming that these are involved in a 2(T) to 1(T) transition.

The populations of the different states at different pressures can be calculated from the corresponding thermodynamic parameters (Figure 1). At atmospheric pressure, states 2(T) and 1(T) dominate, with increasing pressure the population of the effector binding state 2(T) decreases and those of 1(T) first slightly increases and decreases at a pressure larger than 100 MPa. State 3(T) strongly increases, dominates at a pressure of 120 MPa, and decreases again at higher pressure. At pressures of higher than 300 MPa, the population of the nucleotide-free exchange state 1(0) dominates.

Classical rational drug design focuses on the active center of enzymes using small compounds that mimic the substrate(s) or product(s) of the enzymatic reaction. Usually, the enzymatic reaction is inhibited and the drug binds in a competitive way. A special case is the existence of a regulatory site on the enzymes that can also be targeted

by small compounds competing with the natural regulators. The Monod–Wyman–Changeux model (MCW model) of allostery[18] can be reduced to two fundamental conditions, the existence of two structural states of a protein that has 1) two spatially separated binding sites for two different ligands with 2) different affinities in the two states.

As we show, this idea can also be applied to proteins that have not evolved specialized regulatory sites. When a protein interacts with different proteins in a functional cycle, different structural states are required for the specific recognition of the partners (see also Figure 1). In general, these structural differences are not restricted to the interaction site itself, as our high pressure data shows for activated Ras. These structural differences outside the overlapping protein binding sites create "intrinsic" allosteric binding sites that can potentially be recognized selectively by small ligands (condition 1). If the ligand has differential affinities to a given state (condition 2), its binding will increase the relative population of this state and simultaneously influence the populations of all other states.

In fact, we have shown earlier that a stabilization of state 1(T) of Ras by Zn^{2+}-cyclen[12,19,20] can lead to an effective inhibition of effector binding. Zn^{2+}-cyclen binds to the γ-phosphate of GTP inside the nucleotide binding cleft (Figure 2) in a local conformation that only occurs in state 1(T). However, any other binding site for small molecules outside the nucleotide binding cleft can be utilized as long as it is coupled to the 1(T) structural transition. In agreement with this consideration, Zn^{2+}-BPA binds outside the nucleotide binding site but nevertheless is able to stabilize state 1(T).[13] It interacts with Ser39, a residue also sensing the weak nucleotide binding state 1(0) (Figure 3; Supporting Information, Figure S6). In fact, at higher concentrations, Zn^{2+}-BPA induces the release of the bound nucleotide, a property expected for a shift to state 1(0).[13]

The new type of allosteric inhibition has also additional "side" effects, as the stabilization of any state in the signaling cycle shifts the total equilibrium distribution of all other functional states. For Ras, it can be predicted from Figure 1 that Zn^{2+}-cyclen decreases the intrinsic GTPase activity, increases the intrinsic exchange activity but is also expected to decrease the Sos-mediated exchange activity. The latter effect was observed by a group of compounds published by Maurer et al.[14] as Sos inhibitors. Some of these compounds are commercially available, and in fact ^{31}P NMR spectroscopy shows that they are also weak stabilizers of state 1(T) (Supporting Information, Figure S8), although their main function is assumed to focus on the GDP-bound state (perhaps as state 1(D)-stabilizers). Obviously, mixed types of interactions are also possible and likely when an allosteric inhibitor binds at the protein–protein interaction site and thus simultaneously inhibits directly a protein–protein interaction. This is true for Zn^{2+}-BPA, the binding site of which overlaps with the effector binding site of Ras and for the compounds described by Maurer et al.[14] and Sun et al.,[15] the binding sites of which overlap with the binding sites of Sos (Figure 2).

The structure of state 1(T) as it is found in the Ras mutants Ras(T35A) or Ras(T35S) has already been used in experimental[13,21] and virtual[22] drug screening. High-pressure NMR spectroscopy is a powerful method to detect conformational states that can be targeted by small molecules. Additional interesting regions of the surface outside of the protein–protein interaction sites for allosteric inhibition are revealed by high-pressure NMR (Figure 2) that could also be exploited in future.

In summary, this "non-classical" type of allosteric interference provides a generally applicable strategy for the modulation of protein–protein interactions by small compounds, independent of the existence of classical allosteric regulatory sites.

Received: July 3, 2013
Revised: August 20, 2013
Published online: November 11, 2013

Keywords: allosteric inhibition · conformational states · drug design · high-pressure NMR spectroscopy · Ras protein

[1] J. L. Bos, *Cancer Res.* **1989**, *49*, 4682 – 4689.
[2] A. Wittinghofer, H. Waldmann, *Angew. Chem.* **2000**, *112*, 4360 – 4383; *Angew. Chem. Int. Ed.* **2000**, *39*, 4192 – 4214.
[3] H. R. Kalbitzer, M. Spoerner, P. Ganser, C. Hosza, W. Kremer, *J. Am. Chem. Soc.* **2009**, *131*, 16714 – 16719.
[4] M. Geyer, T. Schweins, C. Herrmann, T. Prisner, A. Wittinghofer, H. R. Kalbitzer, *Biochemistry* **1996**, *35*, 10308 – 10302.
[5] M. Spoerner, C. Herrmann, I. Vetter, H. R. Kalbitzer, A. Wittinghofer, *Proc. Natl. Acad. Sci. USA* **2001**, *98*, 4944 – 4949.
[6] M. Spoerner, A. Nuehs, P. Ganser, C. Herrmann, A. Wittinghofer, H. R. Kalbitzer, *Biochemistry* **2005**, *44*, 2225 – 2236.
[7] M. Geyer, C. Herrmann, S. Wohlgemuth, A. Wittinghofer,, H. R. Kalbitzer, *Nat. Struct. Biol.* **1997**, *4*, 694 – 699.
[8] W. Gronwald, F. Huber, P. Grünewald, M. Spörner, S. Wohlgemuth, C. Herrmann, A. Wittinghofer, H. R. Kalbitzer, *Structure* **2001**, *9*, 1029 – 1041.
[9] B. K. Linnemann, M. Geyer, B. K. Jaitner, C. Block, H. R. Kalbitzer, A. Wittinghofer, C. Herrmann, *J. Biol. Chem.* **1999**, *274*, 13556 – 13562.
[10] M. Rohrer, T. F. Prisner, O. Brügmann, H. Käss, M. Spoerner, A. Wittinghofer, H. R. Kalbitzer, *Biochemistry* **2001**, *40*, 1884 – 1889.
[11] J. Koehler, M. B. Erlach, E. Crusca, Jr., W. Kremer, C. E. Munte, H. R. Kalbitzer, *Materials* **2012**, *5*, 1774 – 1786.
[12] I. C. Rosnizeck, T. Graf, M. Spoerner, J. Tränkle, D. Filchtinski, C. Herrmann, L. Gremer, I. R. Vetter, A. Wittinghofer, B. König, H. R. Kalbitzer, *Angew. Chem.* **2010**, *122*, 3918 – 3922; *Angew. Chem. Int. Ed.* **2010**, *49*, 3830 – 3833.
[13] I. C. Rosnizeck, M. Spoerner, T. Harsch, S. Kreitner, D. Filchtinski, C. Herrmann, D. Engel, B. König, H. R. Kalbitzer, *Angew. Chem.* **2012**, *124*, 10799 – 10804; *Angew. Chem. Int. Ed.* **2012**, *51*, 10647 – 10651.
[14] T. Maurer, L. S. Garrenton, A. Oha, K. Pitts, D. J. Anderson, N. J. Skelton, B. P. Fauber, B. Pan, S. Malek, D. Stokoe, M. J. C. Ludlam, K. K. Bowman, J. S. Wu, A. M. Giannetti, M. A. Starovasnik, I. Mellman, P. K. Jackson, J. Rudolph, W. R. Wang, G. Fang, *Proc. Natl. Acad. Sci. USA* **2012**, *109*, 5299 – 5304.
[15] Q. Sun, J. P. Burke, J. Phan, M. C. J. Burns, E. T. Olejniczak, A. G. Waterson, T. Lee, O. W. Rossanese, S. W. Fesik, *Angew. Chem.* **2012**, *124*, 6244 – 6247; *Angew. Chem. Int. Ed.* **2012**, *51*, 6140 – 6143.
[16] E. F. Pai, U. Krengel, G. A. Petsko, R. S. Goody, W. Kabsch, A. Wittinghofer, *EMBO J.* **1990**, *9*, 2351 – 2359.

[17] Y. Ito, K. Yamasaki, J. Iwahara, T. Terada, A. Kamiya, M. Shirouzu, Y. Muto, G. Kawai, S. Yokoyama, E. D. Laue, M. Walchli, T. Shibata, S. Nishimura, T. Miyazawa, *Biochemistry* **1997**, *36*, 9109 – 9119.
[18] J. Monod, J. Wyman, J. P. Changeux, *J. Mol. Biol.* **1965**, *12*, 88 – 118.
[19] H. R. Kalbitzer, B. Koenig, PCT Int. Appl. 14 pp. WO2004006934 A2 20040122, 2004 [CAN 140:122769; AN2004:6032; DE 102 39 612 A1 2004.01.29].
[20] M. Spoerner, T. Graf, B. König, H. R. Kalbitzer, *Biochem. Biophys. Res. Commun.* **2005**, *334*, 709 – 713.
[21] F. Schmidt, I. C. Rosnizeck, M. Spoerner, H. R. Kalbitzer, B. König, *Inorg. Chim. Acta* **2011**, *365*, 38 – 48.
[22] S. Kreitner, M. Spoerner, S. Dove, B. König, H. R. Kalbitzer, Proceedings of the 32th Annual Discussion Meeting of the GDCh Magnetic Resonance Division: Magnetic Resonance in Chemistry and Biology, Münster **2010**, 87 – 87.

